MEASUREMENTS OF LATERAL NOISE EMISSION OF A RAIL WITH A CUSTOM DEVICE

Andrea Bracciali, Gaetano Cascini
Dipartimento di Meccanica e Tecnologie Industriali
Università degli Studi di Firenze
via Santa Marta 3, 50139 Firenze, Italy

Phone: +39 55 4796395
Fax: +39 55 4796400
E-mail: bracciali@ing.unifi.it, cascini@ing.unifi.it

ABSTRACT:

In this work a simplified device for the measurement of the noise emitted laterally by an UIC 60 rail is presented. It consists of three convergent parallel ducts with anechoic termination that collect the sound energy in a straight, cross-square section pipe where measurement microphones are located.

The acoustic design of the device is detailed with reference to the shape definition, based on FEM analysis, and the optimization of the multilayered anechoic termination with experimental and numerical techniques. Laboratory tests performed to calibrate and to validate the device are shown and its acoustical performances are analyzed and discussed.

The overall dimension and the very limited weight of the device ensures the portability and hence its practical use; the limited cost and the use with standard instrumentation make it possible its use for the dectection of rolling surfaces excessive wear.

The results of the first application of the device on a line without macroscopical defects on the rail are shown. A comparison is made between the noise emitted by the rail head, the rail web and the rail foot at the passage of damaged/not damaged wheels.

KEYWORDS:

railway noise, rail, noise measurement, noise measurement custom device, horn, railway wheels wear

1. INTRODUCTION

The different contribution of rail and wheel to global railway noise is a fundamental topic in all railway noise generation and propagation analyses. Several authors dealt with the question and comprehensive reference lists can be found in the proceedings of the past IWRN workshops. The main engineering problem is the intrinsic difficulty in measuring the two sources separately: the contact zone is very limited in space, and the speed of the train is anyway too high not to result in a very limited in time local emission. The problem has been approached by several researchers by looking for acoustical measurements set-up capable to "follow" the moving train: between these, the development of methods using array of microphones are certainly fundamental. All of them are based on advanced techniques using several microphones that perform a sweep, that is moreover capable to eliminate the frequency shift (Doppler effect) due to the train speed; the results are very significant from an engineering point of view, because they allow the localization of the sources on a line or on a plane. On the other side these systems are inevitably quite complicated both on the instrumentation side and on the software post-processing side.

The authors developed in the past few years a custom device to measure noise under the axlebox of any rolling stock [1÷3]. This device in insensitive to air flow and allowed fast and reliable measurements up to 300 km/h. Obviously the axlebox area is fulfilled by several objects (primary suspension springs, axlebox body and guiding links, dampers) and this force the application of the device just under the axlebox, where the measured noise is a combination of rail and wheel emitted noises.

In this paper a new device to measure the noise emitted only by the rail is proposed. It is made of three parallel converging ducts that allows to separately measure the noise emitted by the head, the web and the foot of an UIC 60 rail. Several constraints (acoustical and mechanical) that had to be faced to obtain a reliable device are briefly described; later some results of the first application of the device are presented and discussed.

2. ACOUSTICAL DESIGN OF A NOISE COLLECTOR

The collection of noise emitted by a vibrating surface contrasts with the requirements of knowledge of exact magnitude and phase relationship of the sound emitted by the several portion of the surface. Any collector will, in fact, mix up these components such that the measured sound pressure level will only be meaningful from an energetical point of view. Despite this heavy limitation, such a device proves nonetheless extremely useful in all such situations where the application of more conventional techniques is not possible. Between the latter the array of microphones and the sound intensity techniques can be usefully complemented by the noise collector, the first mainly for cost reasons and both for the application in highly reactive fields where the isolation of the real component of sound intensity proves very hard.

The noise collector partially overcomes another typical problem in the measurement of non stationary noises, namely the duration of the noise emission. For purely random noise sources, and with a good approximation also for wide band noise sources, the relationship that links the bandwith B of the analog or digital filter and the integration time T is such that $BT>1$ must hold. Where transient phenomena are very fast, the sweeping techniques are obviously the best, but also the artificial increase of the measurement duration by collecting the noise from a larger portion of the emitter can help.

2.1 Definition of the shape

The propagation of a plane wave along a cylindrical duct with continuously variable cross section (horn) is governed by mass and energy conservation equation and by the choice of the thermodynamic transformation the fluid undergoes (typically an isentropic one). The differential equation that results can

be solved only for some duct shapes particularly simple, like a conical or exponential horn [4, 5]. For the latter case, the cross section is function of the abscissa z of the horn and of the inlet cross section S_0 with the law $S=S_0e^{mz}$ and the impedance seen from the inlet section is given by

$$Z = \rho c \left(\sqrt{1-\frac{m^2}{4k^2}} + j\frac{m}{2k} \right)$$

(1)

where $k = \omega/c$, c is the sound speed in the air, and $f_c=mc/2\pi$ defines the so-called *cut-off frequency*, below which no sound power is transmitted along the horn. In this case in fact the impedance is everywhere purely reactive and a loudspeaker in the inlet section would not be able to radiate sound power at the outlet section.

Authors did not find in the literature general analytical solutions for collecting (and not radiating) horns where the incoming wave is not plane but generic. Moreover the use of non-circular cross-section horns is even more unusual, as the cylindrical symmetry allows to maximize the sound power emitted (that is the normal situation for loudspeakers!) above the cut-off frequency and reduces the analytical problem to a monodimensional one. The noise collector developed in this research has a rectangular cross-section with constant height; to evaluate to a first degree of approximation wether the chosen dimensions (30×5 cm at the inlet, 5×5 cm at the outlet, lenght of the horn = 35 cm) can be a good basis for the development, the impedance seen by a plane wave entering the duct with an equivalent circular cross-sections was calculated, showing a dramatic increase below 100 Hz, a frequency considered sufficient. The 5×5 cm outlet section is such that plane waves can develop, with appropriate length after the converging duct, up to 3400 Hz without the rise of lateral acoustical eigenmodes. Clearly this approximation is too rough to be retained without further investigation, and extensive simulations have been made by using a FEM code with acoustic capabilities [6]. Three shapes of the rectangular duct where tested, namely linear, cubic and exponential. The shapes and a sketch of the linear horn are shown in fig. 1 where, at the end of the straigth duct, the anechoic termination described in the following must be added. It has been taken into account in the FEM simulation by imposing an absorption coefficient of $\alpha=0.9$.

The simulation has been performed in 2-D and in 3-D with the boundary conditions shown in fig. 2. Noise sources are monopoles with random amplitude in the range 113±2 dB (ref. 20 μPa) and random phase, placed at 30 mm from the inlet section. Acoustical finite elements dimensions are such that there are at least 20 elements per wavelenght at the higher frequencies, condition that proved to be fundamental to obtain sufficiently stable results [7].
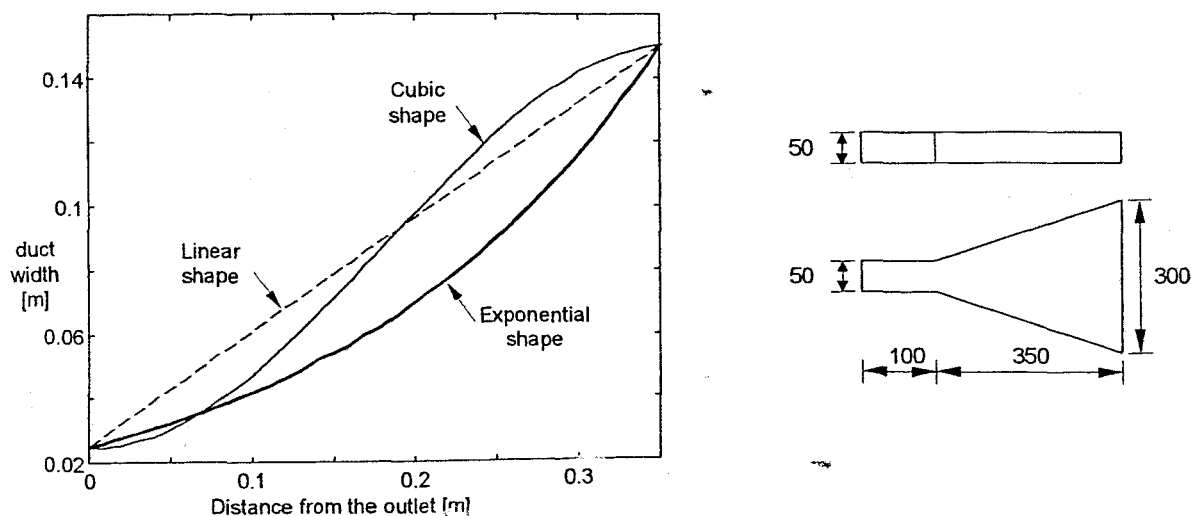

Fig. 1. Lateral shapes used in numerical simulations (left) and overall dimensions for linear-shaped duct (right).

The fast 2-D simulations allowed to prove that the 1/12 octave bands in the range 125 Hz ÷ 4 kHz are almost insensitive to the shape, and that there is no reason to complicate the practical construction of the horn. This can be easily justified recalling that the inlet wavefront is not plane, that the cross section is not cylindrical and that the duct is convering and not diverging. Behaviours shown in fig. 2 are very flat up to 3.4 kHz where lateral resonances take importance.
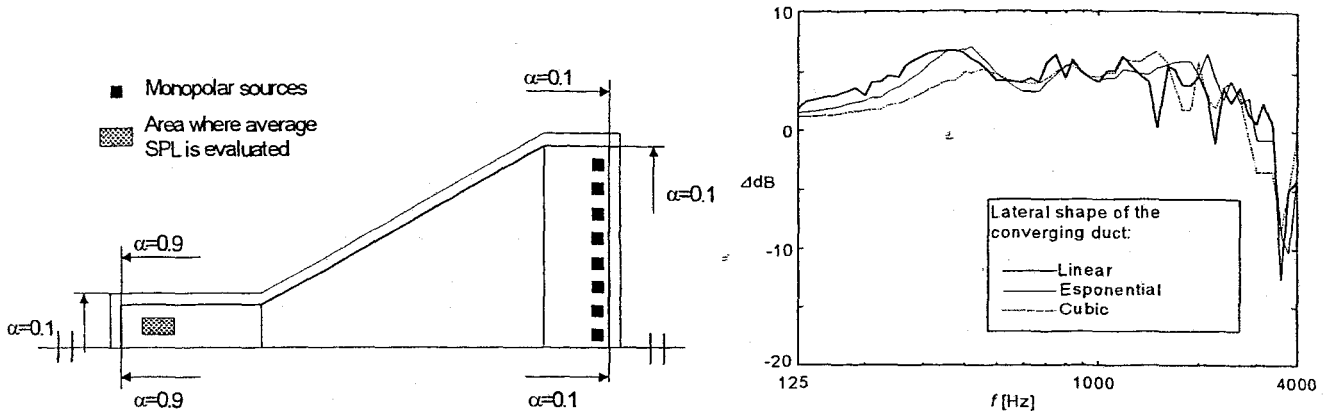

Fig. 2. 2-D FEM model with boundary conditions for linear shape duct (left); SPL calculated in the averaging area normalised w.r.t. the average inlet SPL for the three duct shapes (right).

Three-dimensional simulations are very heavier and did not lead to different results, such that the bi-dimensionality hypothesis can be retained with a very good degree of approximation. An example of the comparison of 2-D and 3-D results is shown in fig. 3.
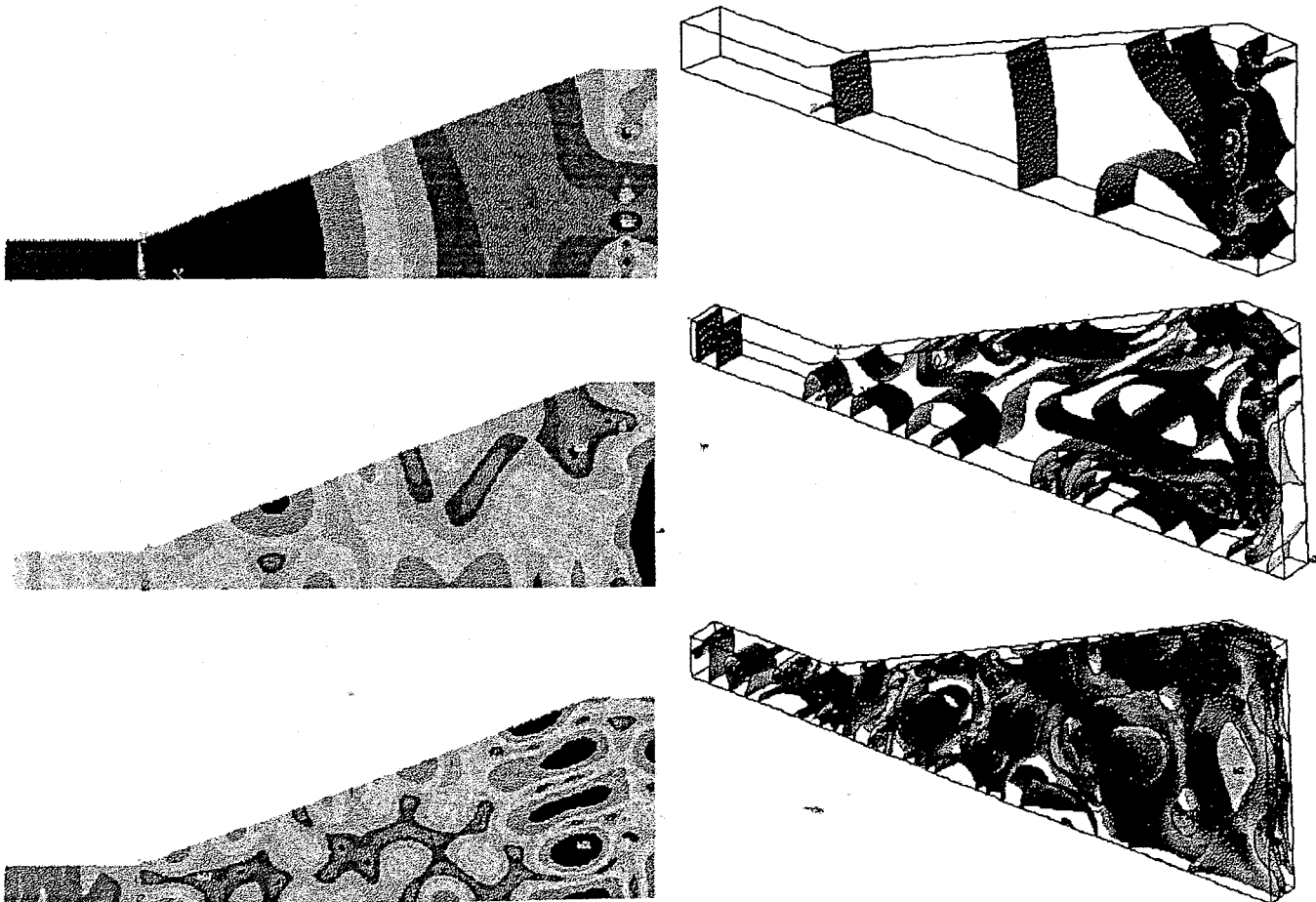

Fig. 3. 2D and 3D iso-SPL surfaces at f=500 Hz (top), f=2920 Hz (mid) and f=5000 Hz (bottom).
Plane wave develops in the cross-squared section up to 3.4 kHz, above which the wave in no more plane.

177

2.2 Optimization of the anechoic termination

The necessity of an anechoic termination is easily understood when considering that only this condition, together with the plane wave condition already seen, allows the measurement of the noise in the straight pipe by means of a single microphone flush-mounted. The only way to efficiently absorb a plane wave broad-band noise is to stack a number of layers of sound absorbing porous materials [8]. The determination of the length and of acoustical properties of the layers is not trivial, apart from the physical and intuitive consideration that flow resistance should increase and layer length should decrease in the direction of the travelling wave. The optimization obviously require some constraints: the overall length of the termination (that must be portable), the maximum number of layers (limited to 3 or 4 materials), the minimum thickness of each layer (very low thicknesses are hardly handled), the frequencies or the frequency range where the absorprion coefficient α must be optimized (it is quite easy to obtain $\alpha=1$ at a particular frequency but this reduces α at the other frequencies), the model of the porous materials to be used (many models with different complication and degrees of accuracy can be used) and, last but not least, the real availability of trade materials (that often must be characterised to obtain the flow resistance $R(f)$, tipically in the range $1000\div80000$ rayls/m).

The overall length has been fixed to 300 mm with a maximum of three layers each with a minimum thickness of 20 mm. The frequencies chosen for the optimization are the multiples of 100 Hz up to 800 Hz, above which α is almost unitary for any possible stratification. The classical and relatively simple Delany and Bazley model for porous materials proved to be sufficiently correct in the flow resistance and density ranges of the materials used. As an analytical solution readily proves to be impossibile as the inversion of a matrix (that is a product of several matrices) that contains hyperbolic functions is impossible, numerical simulations have been made with the use of the MATLAB Optimization Toolbox.

The optimization procedure consists of several steps:

1. a first simulation has been made to estimate the best properties of the materials, by leaving as converging parameters the lengths of the layers l_i and the flow resistances R_i;
2. a selection of commercial materials and their test have been made to cover the possible range of flow resistances R required, after which the materials with R closer to those given by step 1 have been chosen;
3. a second simulation has been made to find the final configuration, fixing the flow resistances R_i and leaving as converging parameters *only* the lengths of the layers l_i;
4. the final experimental verification of the properties of the termination.

The acoustical impedance Z is defined as the ratio of the sound pressure and the velocity of the particle with the $Z=p(x,t)/u(x,t)$. For the air $Z_{air}=\rho c=400$ rayls, where ρ is the air density and c is the sound speed in the air. The properties that define the behaviour of a sound absorbing material with respect to an incident plane wave are the normal incidence propagation constant γ_0 and the normal impedance Z_0 that are given, in the Delany e Bazley model [5], by

$$Z_0 = \rho c[1+0.0571(\rho f/R)^{-0.754}] - j\rho c[0.0870(\rho f/R)^{-0.732}] \qquad (2')$$
$$\gamma_0 = k[0.189(\rho f/R)^{-0.595}] + jk[1+0.0978(\rho f/R)^{-0.700}] \qquad (2'')$$

where the flow resistance R is defined as the pressure drop resulting in a 1 m/s airflow given by a 1 m thick specimen. The acoustical variables upstream and downstream the arbitrary element i along a pipe can be related with the transfer matrix (or four pole parameters) method that, for a multilayer termination, gives the global transfer matrix between upstream element 1 and downstream element N (fig. 4) by partial matrices multiplication:

$$\begin{Bmatrix} p_i \\ u_i \end{Bmatrix} = \begin{bmatrix} T_{11} & T_{12} \\ T_{21} & T_{22} \end{bmatrix} \begin{Bmatrix} p_{i+1} \\ u_{i+1} \end{Bmatrix} = [T] \begin{Bmatrix} p_{i+1} \\ u_{i+1} \end{Bmatrix} \implies \begin{Bmatrix} p_1 \\ u_1 \end{Bmatrix} = \prod_{i=1}^{N} [T] \begin{Bmatrix} p_{N+1} \\ u_{N+1} \end{Bmatrix} = [T] \begin{Bmatrix} p_{N+1} \\ u_{N+1} \end{Bmatrix} \qquad (3)$$
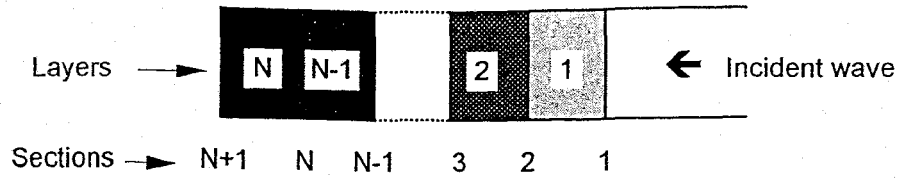
Fig. 4. Layers and sections numbering for a multilayer anechoic termination.

For distributed porous elements the transfer matrix is given by

$$\begin{Bmatrix} p_i \\ u_i \end{Bmatrix} = \begin{bmatrix} \cosh(\gamma_i l_i) & Z_i \sinh(\gamma_i l_i) \\ \dfrac{1}{Z_i} \sinh(\gamma_i l_i) & \cosh(\gamma_i l_i) \end{bmatrix} \begin{Bmatrix} p_{i+1} \\ u_{i+1} \end{Bmatrix} = [T]_i \begin{Bmatrix} p_{i+1} \\ u_{i+1} \end{Bmatrix} \tag{4}$$

For a rigid end $u_{N+1}=0$, and then the inlet impedance is given by

$$\begin{Bmatrix} p_1 \\ u_1 \end{Bmatrix} = \begin{bmatrix} T_{11} & T_{12} \\ T_{21} & T_{22} \end{bmatrix} \begin{Bmatrix} p_{N+1} \\ 0 \end{Bmatrix} \Rightarrow Z_1 = \frac{p_1}{u_1} = \frac{T_{11}}{T_{21}} \tag{5}$$

We remind that the reflection coefficient r_1 and the absorption coefficient α_1 for the inlet section are given by:

$$r_1 = \frac{Z_1 - \rho c}{Z_1 + \rho c} \quad ; \quad \alpha_1 = 1 - |r_1|^2 \tag{6}$$

No details are given here about the experimental setup and procedures necessary to test the various materials and the assembled termination, as they are made with a measurement chain that closely follows the norm ASTM 1050-86 [9] (Kundt pipe).

As a preliminary step it has been verified that the assumed model with the measured properties of some materials can correctly simulate the behaviour of a multilayered termination.

The goal function has been defined as $f(s_i, R_i) = \max(\Sigma \alpha(f))$, where f is the vector of frequency previously mentioned. The materials have then been chosen and a further optimization has been made with the modified goal function $f(s_i) = \max(\Sigma \alpha(f))$, as the flow resistances R_i were fixed. Obtained numerical results are extremely good: $\alpha > 0.8$ at 125 Hz, while $\alpha > 0.95$ for $f > 210$ Hz. Experimental results completely confirm the simulation, and the results are compared in fig. 5.
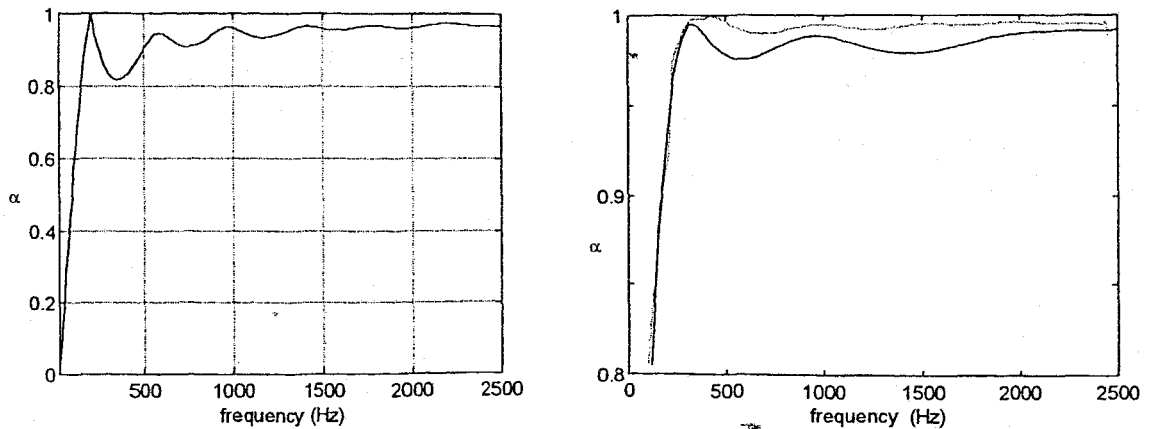

Fig. 5. Absorption coefficient for three layers with $s_1=260$ mm, $R_1=1400$ rayls/m, $s_2=76$ mm, $R_2=3200$ rayls/m, $s_3=63$ mm, $R_3=6000$ rayls/m. Optimization at the frequency $f=200$ Hz (left). Measured (---) and simulated (—) α for the optimal solution with three layers with $s_1=140$ mm, $R_1=1500$ rayls/m, $s_2=100$ mm, $R_2=3500$ rayls/m, $s_3=60$ mm, $R_3=20000$ rayls/m. Optimization at the frequencies $f=100, 200, 300, 400, 500, 600, 700, 800$ Hz (right).

2.3 Experimental validation of the noise collector

The prototype of the noise collector has been made of plywood covered with a hard layer to give a high reflection coefficient to internal walls (fig. 6). The validation of the device has been made through the measurement of the transfer function between two microphones, one inside the straight pipe and the other external to the collector in a position uninfluenced by the collector itself. The measurements have been taken in an acoustical free field with white noise up to 3.2 kHz generated by a loudspeaker 6 m far from the device. The magnitude of the transfer function is particularly low (< 5 dB) confirming the FEM predictions. It must be noted that in a free field the SPL decreases by 6 dB with doubling the distance from the source or, equivalently, the sound pressure decreases by a factor $2^{1/2}$ doubling the area. In the noise collector the ratio between the inlet and outlet area is equal to 6, and so a 9 dB increase in the SPL is expected. The comparison of the 1/3 octave band SPL measured by the microphones confirms this prediction well (fig. 6).
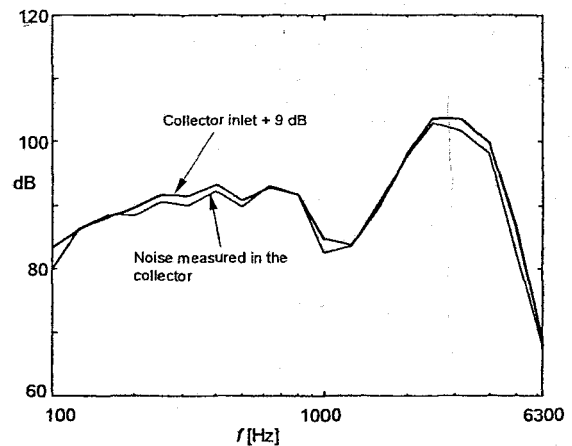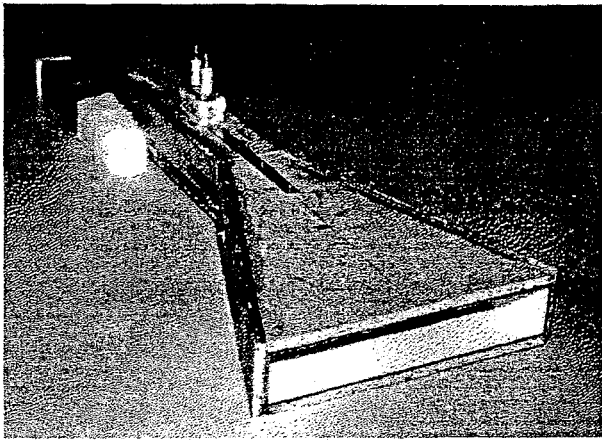

Fig. 6. Prototype of the noise collector with materials used for anechoic termination (left) Comparison of inlet and measured inside the collector sound pressure levels. The SPL outside the collector has been increased by 9 dB to easy the comparison (right).

3. THE TRIPLE HORN FOR THE MEASUREMENT OF LATERAL UIC 60 RAIL EMISSION

The design of the device to be applied to the UIC 60 rail required some precautions. First of all the triple horn is subjected to a very high external noise coming from the passing wheel, and hence it must be made of sound insulating material. Moreover it results to be attached to a structure that moves by several mm and that vibrates with very high levels, and the surfaces of the triple horn can themselves generate noise. At last cross-talk phenomena must be avoided as more as possible, such that the noise measured by a microphone is not influenced by the noise present in the other ducts.

The cross-section of the final solution is shown in fig. 7. UIC 60 rail is 172 mm high; the three ducts are made with "silent steel", i.e. a sheet composed by two steel sheets with a viscoelastic material glued between them (constrained layer technique). This is sufficient to prevent high noise generated by the vibrating surfaces of the triple horn, but to reach sufficiently high values for sound insulation from external noise and to minimize cross-talk problem a double 2 mm silent steel sheet was used, reaching a total height of 174 mm. The inlet sections have been properly extended to match the UIC 60 rail profile as can be seen in fig. 7, where general views in the lab and during the measurement campaign are also shown. The airgap between the inlet section and the rail has been sealed with plaster, a classical solution in experimental acoustics that proved here to be irreplaceable given the high quasi-static deformations of the rail. In the practice the solution demonstrated its validity, as plaster remodelling was not necessary even after the passing of numerous trains.
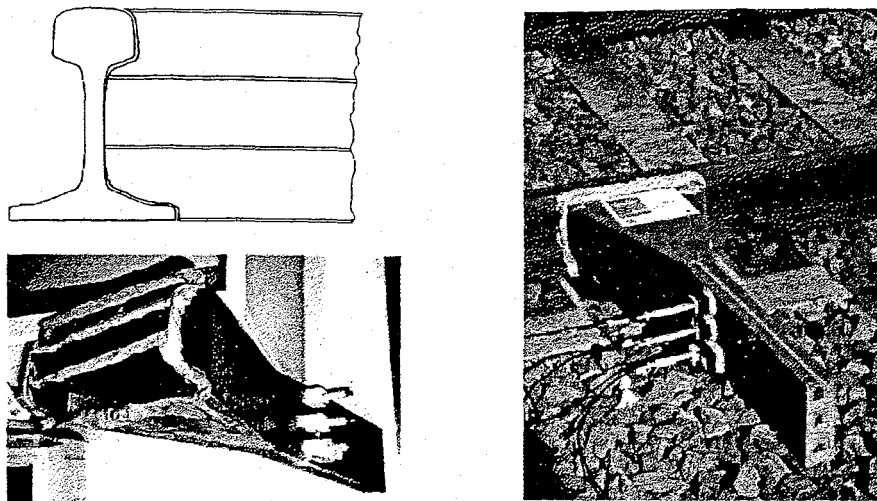
Fig. 7. Sketch of the triple horn (top left), view in the lab (bottom left) and application along the railway line (right).

4. MEASUREMENT DESCRIPTION AND RESULTS

Tests on the noise emitted by the head, the web and the foot of an UIC 60 rail were performed in February 1998 during a noise and vibration measurement campaign on a test site on the railway line outside the Firenze Santa Maria Novella station towards Rome. Several kind of passenger trains run on this line at speeds in the range 10÷25 m/s. There were no macroscopical defects on the rail, but many trains wheel were locally (wheelflat) or globally (polygonization) damaged.

The measurement chain includes three measuring microphones flush mounted on the straight pipes with their preamplifier and a digital computer equipped with an acquisition card with antialiasing filters and a 16 bit ADC. Fig. 8 shows the different SPL measured in the three ducts of the triple horn for several trains in this speed range. Each train is represented by a group of symbols at its passing speed. The SPL evaluation has been made by extracting from digital recording an equivalent length of 1.2 m (twice the distance between two sleepers) centered at the passing of each wheel and taking into account the different time duration for the different speeds. From this diagram it can be seen, not without some graphical difficulties, that the noise increases with speed and that the different parts of the rail contribute in different manners to the global noise. In particular, as it will be seen in the following, the web is the less emitting portion, while higher is the contribution of the head and still higher the contribution of the foot. The dispersion of the noise for some trains seems particularly high.
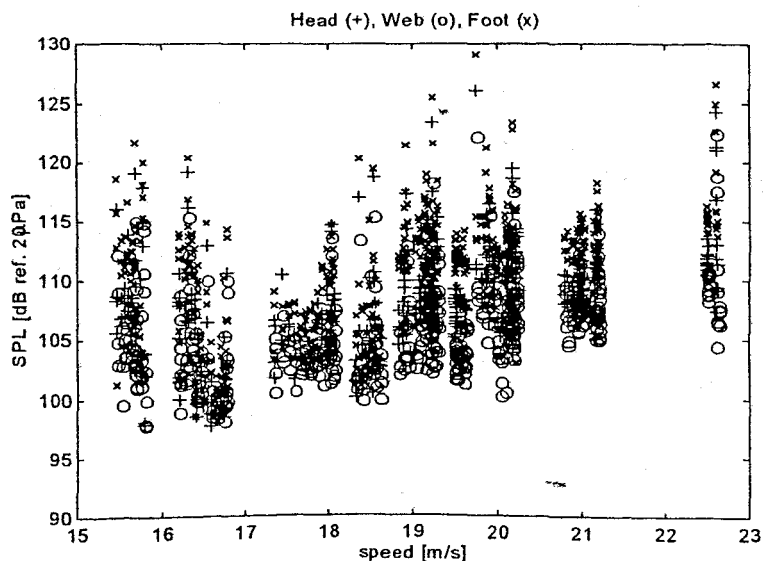

Fig. 8. Corrected average SPL in the inlet section of the triple horn at the passing of all the analyzed wheels on the triple horn mounting section: + head, O web, x foot.

Interesting experimental evidences can be extracted from the analysis of, for instance, the noise measured by the upper horn, namely the one positioned on the head of the rail. Fig. 9a shows the noise measures, corrected with the noise collector constant, for three different trains at the same speed. The fluctuation around the average value are extremely limited for new rolling stock with disc braked wheels with wheels tread in very good conditions, while for some trains in not so perfect conditions the data scattering is decisively higher.

Still more interesting information are obtained by comparing the results for noise levels emitted by the different portions of the rail at the passing of a single train. Data for the typical regional train already seen in fig. 10a are shown in fig. 10b, where it can be seen that the noise emitted by the head is always higher than the noise emitted by the web and lower than the noise emitted by the foot. Defective wheels are clearly recognizable and, especially for these, the contribution of the web can be high (wheel #26), small (wheel #19) or medium (wheel #7). This behaviour is confirmed for all trains with defective wheels.

Constant percentage bandwith frequency analysis for all the wheels of two trains running at the same speed are shown in fig. 10a. The noise emitted by these trains is similar at higher frequencies, but the noise emitted by ETR460 is lower under 400 Hz, presumably because it has a lower wheels roughness.

The analysis of the noise emission at the passing of locally defective wheels (wheelflats) shows (fig. 10b) that not all the portions of the rail are equally sensible to impacts given by this kind of defects. Moreover some band results practically unaffected (see for example the 630÷1600 Hz range) while some others show increases up to 20 dB. Between these frequency bands particularly sensitive results the 1/3 octave band centered at 250 Hz, where all portions of the rail SPL grow up of around 15 dB.
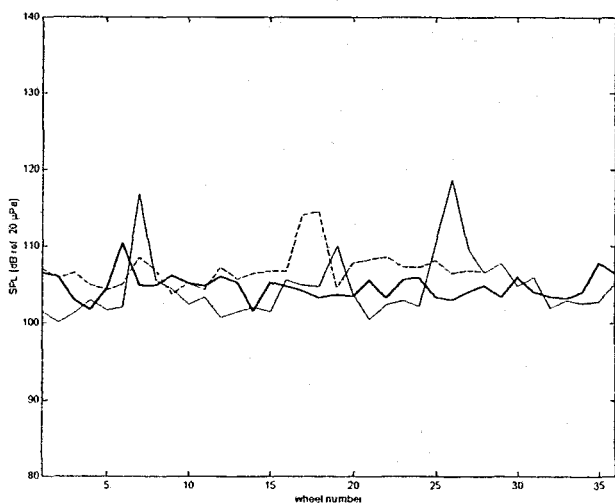

Fig. 9a. SPL measured on the railhead for three trains running at around 18 m/s: thick line ETR 460, thin line 8MD (regional coaches)+D+E652 (loco not shown), dashed line E646+7PR (low floor) (loco not shown)
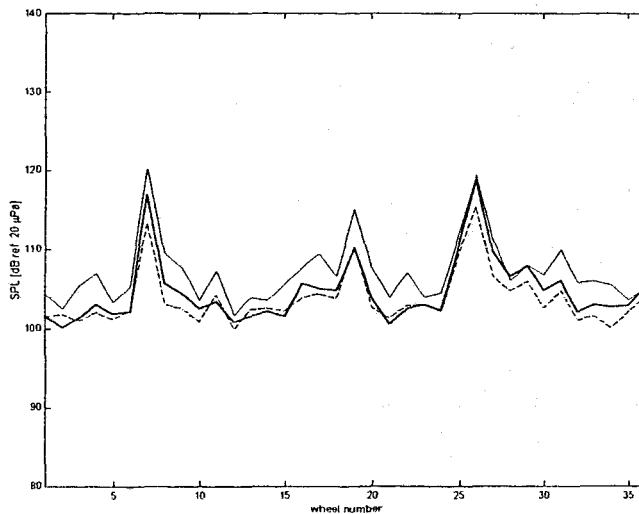
Fig. 9b SPL measured for the train 8MD+B+E652 (loco not shown), 18 m/s (ca.): thick line: railhead, thin line: railfoot, dashed line: railweb

5. CONCLUSIONS AND FURTHER DEVELOPMENTS

The absolutely generic noise collector device briefly described in the first part of this work has been specialized for the measurement of the noise emitted laterally by an UIC 60 rail. The first results obtained are very promising as they allow the direct and economic confirmation of present and future theories on the correct contribution of the rail noise to the global railway noise.

The contemporary measurement of noise on ground with standard methodologies, under the axlebox and on the rail with the devices developed by the authors could be useful to experimentally correctly identify the various sources for many different vehicles with limited costs.
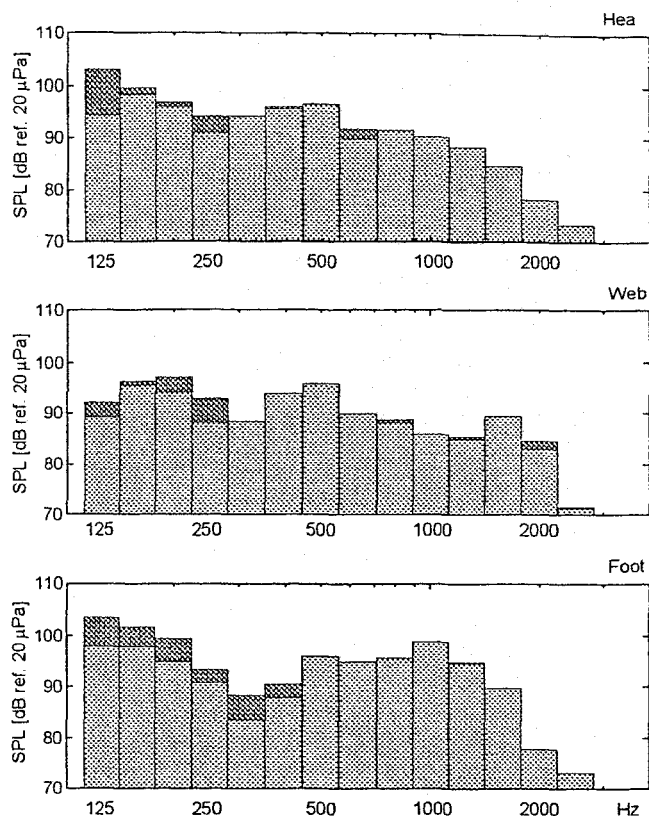
Fig. 10a. Average 1/3 octave band SPL for ETR460 (light) and 8MD+B+E652 (dark) trains. From top: head, web, foot.
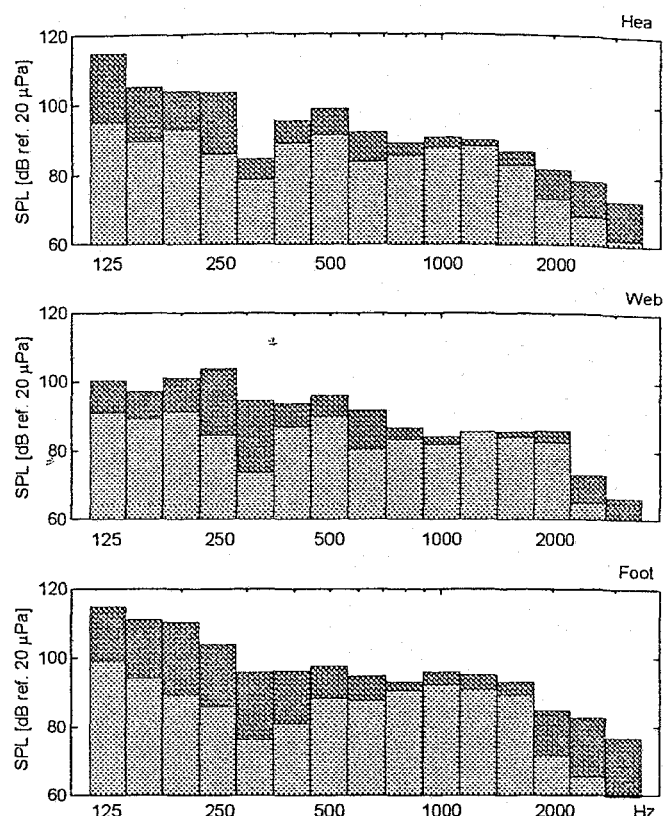

Fig. 10b. 1/3 octave band SPL for 8MD+B+E652 train. Wheel # 6 (not defective – light), wheel # 7 (defective – dark). From top: head, web, foot.

REFERENCES

1. A. BRACCIALI, L. CIUFFI, R. CIUFFI and P. RISSONE 1994 *Journal of Rail and Rapid Transit* **208**, 23-31. Continuous External Train Noise Measurements through an On-board Device.

2. A. BRACCIALI, L. CIUFFI and R. CIUFFI 1994 *Ingegneria Ferroviaria* **6**, 317-332. Metodo Innovativo per la Misura della Rumorosità Esterna dei Convogli Ferroviari.

3. A. BRACCIALI, L. CIUFFI and R. CIUFFI 1997 *Journal of Rail and Rapid Transit* **211**, 41-49. Calibration of an On-Board Noise Measuring Device by Simultaneous Measurement of Trackside Noise of Three Different Wheelsets for the ETR500 F.S. Train.

4. M.L. MUNJAL 1987 *Acoustics of ducts and Mufflers.* New York: John Wiley & Sons.

5. L.L. BERANEK 1971 *Noise and Vibration Control.* New York: McGraw-Hill.

6. ANSYS 1995 *Acoustic and Fluid-Structure Interaction Manuals.* Swanson Analysis System Inc., Houston, PA.

7. A. BRACCIALI and G. CASCINI 1997 *XXV Convegno AIA, Perugia, Italia,* 551-558. Un'attrezzatura per la misura del rumore emesso da una superficie vibrante.

8. A. BRACCIALI and G. CASCINI 1997 *XXV Convegno AIA, Perugia, Italia,* 167-174. Ottimizzazione Acustica di una Terminazione Anecoica.

9. ASTM E 1050-86 *American Society for Testing and Materials, 1916 Race St., Philadelphia, PA 19103.* Standard Test Method for Impedance and Absorption of Acoustical Material using a Tube, Two Microphones and a Digital Frequency Analysis System.